Experimental and topological determination of the pressure-temperature phase diagram of morniflumate, a pharmaceutical ingredient with anti-inflammatory properties

M. Barrio[1,2], J.-Ll. Tamarit[1,2], R. Ceolin[1,2,3], B. Robert[4,†], C. Guéchot[5], J.-M. Teulon[6], I.B. Rietveld[4,7,*]

[1] Grup de Caracterització de Materials, Departament de Física, EEBE, Universitat Politècnica de Catalunya, Campus Diagonal-Besòs, Av. Eduard Maristany 10-14, 08019 Barcelona, Catalonia, Spain.
[2] Barcelona Research Center in Multiscale Science and Engineering, Av. Eduard Maristany, 10-14, Barcelona 08019, Spain
[3] LETIAM, EA7357, IUT Orsay, Université Paris Sud, rue Noetzlin,
91405 Orsay Cedex, France
[4] Normandie Université, Laboratoire SMS - EA 3233, Université de Rouen, F 76821 Mont Saint Aignan, France
[5] Solvay SA, 25, rue de Clichy, 75009, Paris, France.
[6] 78170 La Celle Saint Cloud, France
[7] Faculté de Pharmacie, Université Paris Descartes, USPC, 4 avenue de l'observatoire, 75006, Paris, France

[*] Corresponding author: ivo-boudewijn.rietveld@univ-rouen.fr

[†] Present address: Sanofi R&D, Pharmaceutics Development Platform/Analytical Sciences/Solid State group. 13 quai Jules Guesde, F-94400 Vitry sur Seine, France

ABSTRACT

The pressure-temperature phase diagram of morniflumate (niflumic acid β-morpholinoethyl ester) has been obtained by high-pressure thermal analysis. In addition, calorimetric melting data ($T_{I\rightarrow L}$ = 348.1 ±0.4 K and $\Delta H_{I\rightarrow L}$ = 89 ±2 J g^{-1}) and the specific volumes of the solid and the liquid state have been obtained under normal pressure. Comparison of the measured high-pressure melting data with the equilibrium curve obtained through the Clapeyron equation indicates that the initial slopes are the same (dP/dT = 2.96 ±0.06 MPa K^{-1}) at the melting point under normal pressure. The fact that the Clapeyron equation can be used to construct topological phase diagrams may be of interest for the food and pharmaceutical industries.

Keywords: high-pressure, pressure-temperature phase diagram, Clapeyron, topological phase diagram, specific volume, density

1 INTRODUCTION

Unary pressure-temperature phase diagrams are used in physical chemistry for more than a hundred years and were a popular subject of research at the end of the nineteenth century and the beginning of the twentieth century as can be judged by the contributions from Tammann, Hulett, Bakhuis-Roozeboom, and Bridgman [1-4]. In the meantime, high-pressure research has moved on to ultra-high pressures, even if high-pressure research of molecular substances is important for the understanding of their solid-state behavior. Crystalline polymorphism is an issue in the pharmaceutical and food industry and depends on the thermodynamics of the system. High-pressure measurements can give access to thermodynamic quantities, such as transition temperature, transition enthalpy, and volume change in the system through the Clapeyron equation:

$$\frac{dP}{dT} = \frac{\Delta s}{\Delta v} = \frac{\Delta h}{T\Delta v} \qquad (1)$$

with Δs the specific entropy change associated with the phase transition, Δv the specific volume change, Δh the specific enthalpy change and T the equilibrium temperature (as $T \cdot \Delta s = \Delta h$ is valid at equilibrium). On the one hand, such measurements make it possible to verify enthalpy and specific volume values obtained by calorimetry and X-ray diffraction under ambient pressure conditions, and on the other hand, the Clapeyron equation can be used to calculate the high-pressure behavior of the system [5, 6]. This is in particular interesting for the pharmaceutical industry, when they need to decide to what extent polymorphism may cause problems in the preformulation stage of a drug. However, little is known about the extent the dP/dT slope obtained through the Clapeyron equation can be extrapolated to higher pressure, because few phase diagrams on molecular compounds and active pharmaceutical compounds (APIs) exist. Thus from a practical standpoint, high-pressure phase diagram research reinforces an easy access to the thermodynamic behavior of small molecular compounds, which is directly applicable in industry and from a more academic standpoint, high-pressure data provides inside in general thermodynamic properties such as the specific volume (equation of state) and the entropy of molecular systems under pressure. More experimental data will definitely support the theoretical inroads made to describe the solid and liquid state of molecular substances.

The anti-inflammatory API morniflumate is the β-morpholinoethyl ester of niflumic acid. According to patent EP0349902A2, it "*was described for the first time by C. Hoffmann in French Patent n° 7963M filed on october 1968"* [7]. Esterification of niflumic acid with the β-morpholinoethyl moiety was intended to improve drug tolerability and to reduce injuries of the gastrointestinal mucosa. Solid-state studies indicated that the compound crystallizes in a triclinic structure, which was solved by Toffoli et al in 1988 [8]. The molecular structure based on the crystal structure has been provided in Figure 1. The thermodynamic properties such as the melting temperature, heat of fusion and the specific heat have been investigated by Pinvidic et al. in 1989 [9]. In this paper, the pressure-temperature (P-T) phase diagram of morniflumate is presented and used to investigate the difference between the experimental slope and the slope as determined by the Clapeyron equation. In addition, the required thermodynamic data, such as the melting temperature, the melting enthalpy, and the specific volume of the solid and the liquid will be discussed.

2 EXPERIMENTAL

2.1 Sample

Morniflumate (Figure 1) of medicinal grade, manufactured by Archimica SAS, France, obtained from UPSA laboratories was used as provided after verification by X-ray and DSC. The certificate of analysis from Archimica SAS indicated a purity higher than 99% with a content in free niflumic acid of 0.1% (m/m).

2.2 Differential Scanning Calorimetry (DSC)

Temperature (onset) and heat of fusion were obtained with two Q100 thermal analyzers from TA Instruments at different sites with various heating rates. The analyzers were calibrated by using the melting point of indium (T_{fus} = 429.75 K and $\Delta_{fus}H$ = 3.267 kJ mol^{-1}). Specimens were weighed using a microbalance sensitive to 0.01 mg and for the second DSC sensitive to 0.001 mg and sealed in aluminum pans.

2.3 High-resolution X-ray powder diffraction

Two series of XRPD measurements using the Debye–Scherrer geometry and transmission mode were performed with a vertically mounted INEL cylindrical position-sensitive detector (CPS-120). Monochromatic Cu-Kα_1 (λ = 0.154056 nm) radiation was selected by means of an asymmetrically focusing incident-beam curved quartz monochromator. Measurements as a function of temperature were performed using a liquid nitrogen 700 series Cryostream Cooler from Oxford Cryosystems. Cubic phase $Na_2Ca_3Al_2F_4$ was used for external calibration. PEAKOC application from DIFFRACTINEL software was used for the calibration as well as for the peak position determinations after pseudo-Voigt fittings and lattice parameters were refined by way of the least-squares option of the FullProf suite [10, 11].

Specimens were introduced in a Lindemann capillary (0.5-mm diameter) and allowed to rotate perpendicularly to the X-ray beam during the experiments to improve the averaging of the crystallite orientations. Before each isothermal data acquisition the specimen was allowed to equilibrate for about 10 min, and each acquisition time was no less than 1 h. The heating rate in-between data collection was 1.33 K min^{-1}. Patterns were recorded on heating in the temperature range from 100 K up to the melting point.

2.4 Densitometry of the melt as a function of temperature

Liquid density as a function of temperature was measured with a DMA-5000 Density Meter from Anton-Paar. The specimen was introduced in the molten state in the apparatus equilibrated at a temperature above the temperature of fusion. Data were obtained at isothermal steps while slowly cooling in the temperature range from 363 to 323 K. Dry air and bi-distilled water were used as calibration standards in the temperature range. The temperature was controlled at ± 1 mK.

2.5 High-pressure differential thermal analysis (HP-DTA)

HP-DTA measurements have been carried out at 2 K min^{-1} using a home-made high-pressure differential thermal analyzer similar to Würflinger's apparatus and operating in the 298 – 473 K and 0 – 250 MPa ranges [12]. To determine the melting temperature as a function of pressure and to ascertain that in-pan volumes were free from residual air, specimens were mixed with an inert perfluorinated liquid (Galden®, from Bioblock Scientifics, Illkirch, France) as a pressure-transmitting medium, and the mixtures were sealed into cylindrical tin pans. To check that the perfluorinated liquid was chemically

inactive, and should thus have no influence on the melting temperature of morniflumate, preliminary DSC measurements were carried out with a Galden®-morniflumate mixture on a Q100 analyzer of TA instruments without applied pressure.

3 RESULTS

3.1 Calorimetric data

DSC measurements have been carried out with thirteen different samples using heating rates of 0.5, 2, 5, and 10 K min^{-1}. The results of the individual measurements have been compiled in Table S1 in the Supplementary Materials. It has led to a temperature of fusion, $T_{l\rightarrow L}$, of 348.1 K ±0.4 K (standard uncertainty u) obtained from the onset of the melting peak and it has yielded the mean value of 89.4 J g^{-1} ±1.6 J g^{-1} (u) for the melting enthalpy, $\Delta H_{l\rightarrow L}$, a little larger than the value of 87.25 J g^{-1} found previously [9]. Neither the melting point nor the melting enthalpy appear to depend on the heating rate of the DSC. On reheating the melt, a glass transition was observed in agreement with previous findings [9] at T_g = 249.4 K ±0.5 K (u) (midpoint) and no further recrystallization is observed. In Figure 2, the melting peak and the glass transition for the heating rate of 2 K min^{-1} has been provided.

3.2 Specific volume as a function of temperature

3.2.1 Crystalline morniflumate

Two different samples of morniflumate have been measured with X-ray powder diffraction and the lattice parameters as a function of temperature have been calculated. They can be found in the Supplementary Materials Table S2. The resulting unit cell volumes and specific volumes of morniflumate as a function of the temperature have been compiled in Table 1. The specific volumes of the crystalline solid, which have been plotted in Figure 3 were fitted to a quadratic function (v_s /$cm^3 g^{-1}$, T /K, ±u):

$$v_s\,(T) = 0.6778\ (\pm 0.0011) + 5.8\ (\pm 1.0) \times 10^{-5}\ T + 1.7\ (\pm 0.2) \times 10^{-7}\ T^2 \quad (r^2 = 0.999) \quad (2)$$

Table 1. Morniflumate unit cell volume (V_{cell}), which contains two molecules (Z = 2), and specific volume (v_s) as a function of temperature (T) measured in an open system under air with a pressure of 0.1 MPa.[a]

T /K	V_{cell} /10^{-3} nm^3	v_s /cm^3 g^{-1}
First series		
100.0	900.4	0.68570
150.0	907.6	0.69118
200.0	915.01	0.69682
320.0	938.2	0.71445
330.0	939.6	0.71558
335.0	941.6	0.71705
340.0	942.4	0.71766
Second series		
125.0	902.4	0.68720
175.0	910.01	0.69301
225.0	918.60	0.69955
250.0	923.82	0.70353
273.0	927.45	0.70630
298.2	934.34	0.71154
315.0	936.85	0.71346
325.0	938.50	0.71471
332.0	940.94	0.71657
337.0	941.6	0.71711
342.0	943.34	0.71840
347.0	944.39	0.71920

[a]Standard uncertainties are $u(T)$ = 0.2 K, $u_r(P)$ = 0.05, $u(V_{cell})$ = 0.55 ×10^{-3} nm^3 and $u(v_s)$ = 0.0004 cm^{3}g^{-1}.

3.2.2 Liquid morniflumate

The density of molten morniflumate was measured with decreasing temperature every five kelvins from 363 K to 323 K. Results have been compiled in Table S3 in the Supplementary Materials and a linear fit to the temperature dependent specific volume (v_{liq}/cm^{3}g^{-1}, T /K, ±u) has led to:

$$v_{liq}(T) = 0.6045\ (\pm 0.0005) + 0.000579\ (\pm 0.000014) \times T \qquad (r^2 = 0.9999) \qquad (3)$$

The specific volume of the liquid has been plotted in Figure 3 together with the data for the crystalline state.

3.3 High-pressure differential thermal analysis

The melting temperatures observed in seven runs at different pressures ranging from 0 to 250 MPa have been compiled in Table 2. The resulting pressure-temperature melting curve based on the "raw" unrounded data, using T as the running variable and giving P as a function of T, is best described by a straight line (with P in MPa and T in K, ±u):

$$P = -1201\ (\pm 40) + 3.44\ (\pm 0.11)\ T \qquad (R^2 = 0.994) \qquad (4)$$

Table 2. Pressures (*P*) and onset temperatures (*T*) of the melting peaks obtained by high-pressure differential thermal analysis.[a]

P /MPa	T /K
0.1	348.1
32	358.5
58	366.9
79	374.5
115	382.7
140	390.7
155	396.0
201	403.7
244	421.5

[a]Standard uncertainties are $u(T)$ = 0.4 K and $u_r(P)$ = 0.05 for P = 0.1 MPa and $u(T)$ = 1.5 K and $u(P)$ = 1 MPa for P > 0.1 MPa.

4 DISCUSSION

4.1 The thermal expansion of the solid and the liquid

The thermal expansion of the volume of solid morniflumate is best fitted by the quadratic expression eq. 2. However, to compare its expansion with other molecular solids, it is more convenient to determine the thermal expansion coefficient $\alpha_{V,s}$, which is defined by the linear equation $v_s(T) = v_0\ (1+\alpha_{V,s}\ T)$. Fitting the data in Table 1 to the latter equation, leads to 2.09 (±0.04) $\times 10^{-4}$ K^{-1} for $\alpha_{V,s}$ (with v_0 = 0.6695(±0.0008) cm^3g^{-1}) in the temperature range of 100 to 347 K. This is very close to the value of 2.21 $\times 10^{-4}$ K^{-1} previously reported by the present authors for solid molecular active ingredients, which had also been reported by Gavezzotti for solid organic compounds [13-15]. Clearly, morniflumate has a very predictable average thermal expansion in the solid state.

Molten morniflumate has a thermal expansion described by the linear equation 3. Using the same approach to obtain the thermal expansion coefficient of the liquid phase $\alpha_{V,liq}$, 9.58(±0.24) $\times 10^{-4}$ is found, which is somewhat smaller than 1.20(±0.25) $\times 10^{-3}$ K^{-1} found previously for similar compounds, but it is still within the standard deviation of the observed distribution for the thermal expansion of liquids of active pharmaceutical compounds [14, 15].

4.2 Isobaric thermal expansion tensor for the solid

The anisotropy of the intermolecular interactions can be investigated with the isobaric thermal expansion tensor, which is a measure of how the interactions change with temperature [16]. It is the symmetrical second-rank tensor, with nonzero eigenvalues on the diagonal α_1, α_2, and α_3 [17-23]. A small value for a tensor eigenvalue is commonly referred to as a "hard" direction indicating a small deformation and a large value as a "soft" direction indicating a large deformation. For triclinic systems, the eigenvectors are completely independent of the crystal axes **a**, **b**, and **c** and contrary to them, the eigenvectors constitute an orthogonal system.

With the thermal expansion data provided in the Supplementary Materials (Table S2), the isobaric thermal expansion tensor has been calculated. The full results can be found in Table S4 of the Supplementary Materials and a graphic representation of the tensor at 255 K can be found in Figure 4. The eigenvalues increase with the temperature, but are under all circumstances positive. At 300 K, the soft direction of the crystal is

characterized by α_1 with a value of 1.53 $\times 10^{-4}$ and the hardest direction by α_3 with a value of 0.21 $\times 10^{-4}$. The intermediate α_2 has a value of 0.54 $\times 10^{-4}$. The aspherism coefficient (symbol A in Table S4 in the supplementary materials) indicative for the measure of anisotropy in the thermal expansion is in the order of 0.4 (see also the graphical representation of the tensor in Figure 4), but it tends to become smaller with increasing temperature, indicating that the expansion becomes more isotropic (A = 0 representing fully isotropic expansion). The eigenvalues of the tensor are comparable to those of other small organic compounds with therapeutic activity, like L-tyrosine methyl ester, L-tyrosine ethyl ester, and tienoxolol for example [21, 24, 25].

Due to a lack of classical hydrogen bond donors—the only N-H present in the structure is involved in an intramolecular hydrogen bond—the crystal is susceptible to thermal expansion in all directions and in particular the expansion of the hard direction is relatively large in comparison with the examples mentioned just above. On the other hand, it is clear that the soft direction, α_1, is marked by layers of morniflumate molecules that share few close contacts (This has been illustrated in the Supplementary Materials in Figure S1). It may be one of the main causes of the relatively low melting point of morniflumate. The other directions contain some of the weaker types of hydrogen bonds between hydrogens of the aromatic rings as donor and the double bonded oxygen of the ester as acceptor.

4.3 The volume change on melting

On melting, the directional short-range interactions present in the crystalline materials cease to exist and are replaced by more random interactions in the liquid state. Even if the molecules remain close, the random positioning of the molecules in the liquid is in general accompanied by an increase of volume on melting (except for a few special cases such as water). In the case of small organic molecules (100 – 500 g mol^{-1}) to which morniflumate belongs together with many other pharmaceuticals, the volume increase on melting tends to be on average about 10% ± 3% [14, 15], slightly smaller than the 12% based on 21 compounds reported previously by Goodman et al. [26].

Taking the specific volume dependence of the crystalline solid with the temperature (eq. 2) and the temperature of melting of 348.1(±0.4) K, the specific volume of the crystal at the melting temperature can be calculated to be 0.71923(±0.00042) cm^3g^{-1}. The temperature dependence for the liquid (eq. 3) leads to a specific volume at the melting point of 0.80615(±0.00007) cm^3g^{-1}. Thus, the change in specific volume on melting equals 0.08692(±0.00049) cm^3g^{-1} and the ratio v_{liq}/v_s is 1.121(±0.001). The latter ratio is in very good agreement with the volume changes on melting mentioned above.

4.4 The volume difference at the glass transition

The glass transition temperature was found at 249.4 K. At this temperature the undercooled liquid becomes a “solid” kinetically restrained liquid. By extrapolation of eq. 3, the specific volume of the liquid at the glass transition can be estimated and was found to be 0.7490(±0.0004) $cm^3\ g^{-1}$. The crystalline solid at that temperature (eq. 2) has a specific volume of 0.7032(±0.0004) $cm^3\ g^{-1}$. The glass is less dense than the crystalline phase and the difference in specific volume is 0.0458(±0.0008) cm^3g^{-1}. The ratio of the specific volume of the solid over that of the liquid is 1.065(±0.001), disregarding the 1, the decimal values of this ratio are approximately half in comparison with the ratio at the melting point.

The specific volume of the glassy state as a function of the temperature generally levels off strongly and starts to contract like the solid state. If the contraction as observed in the liquid state were to continue, the liquid (or glass) would at a given temperature have the same density as the crystalline phase. This is called the Kauzmann paradox, as it would be impossible that a disordered liquid can have the same specific volume as the ordered crystalline solid [27]. The temperature at which this seemingly occurs is called the Kauzmann temperature, which for this system would be 148 K (see Figure 3). If a glass transition is lacking, the Kauzmann temperature can be considered the extreme minimum temperature, where a liquid phase could exist. Obviously, any experimental glass transition will occur above the Kauzmann temperature.

4.5 The slope of the solid-liquid equilibrium in the pressure-temperature diagram

The slope of a two-phase equilibrium in a pressure-temperature phase diagram is given by the Clapeyron equation (eq. 1). Using the values obtained by calorimetric measurement, one finds that the entropy change, Δs, equals 89.43/348.1 = 0.2569(±0.0047) J g^{-1} K^{-1}. The slope of the melting equilibrium with the volume change calculated above leads to dP/dT = 0.2569/0.08692 = 2.96(±0.07) MPa K^{-1}.

The dP/dT slope calculated with the Clapeyron equation (eq. 1), is rather low in comparison with the experimental value obtained by the high pressure differential thermal analysis, which has led to 3.44(±0.11) MPa K^{-1} (eq. 4) The reason for this difference is most likely related to the curvature of the melting equilibrium, as in most cases the volume of the liquid will change more readily with increasing pressure than the solid. Therefore, the volume change on which the slope of the equilibrium depends as can be seen in the Clapeyron equation (eq. 1) will change to a certain extent with pressure. It may be possible to investigate this using a quadratic function to fit the experimental data in Table 2:

$$P = -892(\pm 695) + 1.8(\pm 3.6)\, T + 2.1(\pm 4.7) \times 10^{-3}\, T^2 \qquad (R^2 = 0.994) \qquad (5)$$

It can immediately be seen that the quadratic function does not capture the curvature of the slope, as its correlation coefficient and that of eq. 4, the linear function, are the same and thus the quadratic function does not improve the fit. Furthermore, the errors over the fitting parameters are larger than their values and they can therefore not be considered statistically sound, even if the overall fit is acceptable. Evaluating the slope at 348.1 K nonetheless, leads to a value of 3.29 MPa/K, thus slightly smaller than that found by the linear equation, however the statistical error is larger than its value and thus it is not possible to compare the slope obtained from eq. 5 with the value obtained by the Clapeyron equation.

This problem is most likely due to the scatter over the measurement points, which make it difficult for the quadratic equation to capture the proper curvature. An alternative is to investigate the change of the slope by fitting a limited number of points to a straight line, starting at zero pressure and one by one adding a melting temperature obtained at a higher pressure. The resulting slopes can be found in Table 3.

Table 3. The evolution of the equilibrium slope with standard uncertainty *u* and its correlation coefficient R^2 based on a linear equation as a function of the number of data points used

Number of data points	Slope (±*u*)	R^2
2	3.05(-)[a]	1[a]
3	3.09(±0.03)	0.99992
4	3.01(±0.05)	0.9994
5	3.25(±0.15)	0.994
6	3.30(±0.11)	0.996
9	3.44(±0.11)	0.994
Clapeyron (eq. 4)	2.96(±0.06)	-

[a] no error with only two data points

It is clear from table 3 that using only a few points to determine the slope of the equilibrium, the value is much closer to the one determined by the Clapeyron equation. As the error over the values determined with only a few points is most likely underestimated, ±0.11 MPa/K can be used as a global error, because this seems to be approximately de limiting error when all P-T data points are used. In that case, the slopes calculated with 2, 3, or 4 data points are within error equal to the value obtained by the Clapeyron equation (for example 3.01 ± 0.11 and 2.96 ± 0.7 MPa/K). So even though due to possible scatter over the experimental data points the curvature of the melting equilibrium cannot not be fitted well with a quadratic function, the foregoing analysis seems to point to a slight curvature. Further evidence that the Clapeyron equation describes the initial slope at 0 MPa well can be found in Figure 5, where the measured data points are plotted together with those obtained through the Clapeyron equation. The points obtained by the Clapeyron equation virtually overlap with the first four high-pressure data points.

5 CONCLUDING REMARKS

The specific volume data obtained for morniflumate confirms the statistics found for the specific volume data of other small molecular compounds. The expansion coefficients in the solid and in the liquid are both close to the statistical averages. In addition, the ratio of the volume change on melting of morniflumate is found to be very close to the average range of 10 to 12 % in volume increase.

It is also clear from the experimental pressure-temperature melting curve that the Clapeyron equation using only the melting enthalpy and temperature obtained by DSC and the specific volumes obtained by X-ray and density measurements provides a good estimate of the initial slope of the melting equilibrium (see Figure 5). It is however important to be able to fit the curvature of the experimental pressure-temperature curve correctly and that may in certain cases not be easy as has been demonstrated by the case of morniflumate. Nonetheless, this paper shows that the Clapeyron equation can be reliably used to construct topological pressure-temperature phase diagrams without the immediate need of measuring systems under pressure. This may be an advantage for the food and drug industries.

Acknowledgments
This work was supported by the Spanish Ministry of Science and Innovation [grant number FIS2014-54734-P] and by the Generalitat de Catalunya [grant number 2014 SGR-581].

The authors declare no conflict of interest. B. R. is an employee of Sanofi, C. G. is an employee of Solvay

Supplementary Materials available: Tables of melting temperature and melting enthalpy at different heating rates, of the lattice parameters of morniflumate as a function of temperature, of the density of liquid morniflumate as a function of temperature, and of the eigenvalues of the isobaric thermal expansion tensor. Figures of the orientation of the expansion tensor in relation to the unit cell.

References

[1] G.A. Hulett, Der stetige Übergang fest-flüssig, Z. Phys. Chem. (Munich) 28 (1899) 629-672.
[2] H.W. Bakhuis Roozeboom, Die heterogenen Gleichgewichte vom Standpunkte der Phasenlehre. Erstes Heft: Die Phasenlehre - Systeme aus einer Komponente., Friedrich Vieweg und Sohn, Braunschweig, 1901.
[3] P.W. Bridgman, Change of phase under pressure I. The phase diagram of eleven substances with special reference to the melting curve, Phys. Rev. 3 (1914) 126-203.
[4] G. Tammann, Aggregatzustände, Voss, Leipzig, 1922.
[5] S. Toscani, R. Céolin, L. Ter Minassian, M. Barrio, N. Veglio, J.-L. Tamarit, D. Louër, I.B. Rietveld, Stability hierarchy between piracetam forms I, II, and III from experimental pressure-temperature diagrams and topological inferences, Int. J. Pharm. 497 (2016) 96-105.
[6] R. Ceolin, S. Toscani, I.B. Rietveld, M. Barrio, J.-L. Tamarit, Pitfalls and feedback when constructing topological pressure-temperature phase diagrams, Eur. Phys. J. - S.T. (2017) in press, doi:10.1140/epjst/e2016-60246-60246.
[7] P. Chiesi, V. Servadio, R. Pighi, Processes for the preparation of morniflumate and analogous compounds. in: E.P. Office, (Ed.), Europe, 1990.
[8] P. Toffoli, M. Coquillay, N. Rodier, R. Ceolin, J.M. Teulon, C. Guechot, Morpholinoethyl Niflumate (DCI: Morniflunate), Acta Crystallogr. C 44 (1988) 547-550.
[9] J.J. Pinvidic, A. Gonthier-Vassal, H. Szwarc, R. Ceolin, P. Toffoli, J.M. Teulon, C. Guechot, Niflumic Acid Morniflumate Phase-Diagram .1. Study of the Components, Thermochim. Acta 153 (1989) 37-45.
[10] J. Rodriguez-Carvajal, Recent advances in magnetic structure determination by neutron powder diffraction, Physica B 192 (1993) 55-69.
[11] J. Rodriguez-Carvajal, T. Roisnel, J. Gonzales-Platas, Full-Prof suite version 2005, Laboratoire Léon Brillouin, CEA-CNRS, CEN Saclay, France, 2005.
[12] A. Würflinger, Differential thermal-analysis under high-pressure IV. Low-temperature DTA of solid-solid and solid-liquid transitions of several hydrocarbons up to 3 kbar, Ber. Bunsen-Ges. Phys. Chem. 79 (1975) 1195-1201.
[13] A. Gavezzotti, Molecular Aggregation. Structure Analysis and Molecular Simulation of Crystals and Liquids, Oxford University Press, Oxford, UK, 2013.

[14] R. Céolin, I.B. Rietveld, The topological pressure-temperature phase diagram of ritonavir, an extraordinary case of crystalline dimorphism, Ann. Pharm. Fr. 73 (2015) 22-30.
[15] I.B. Rietveld, R. Céolin, Phenomenology of crystalline polymorphism: overal monotropic behavior of the cardiotonic agent FK664 forms A and B, J. Therm. Anal. Calorim. 120 (2015) 1079-1087.
[16] J. Salud, M. Barrio, D.O. Lopez, J.L. Tamarit, X. Alcobe, Anisotropy of intermolecular interactions from the study of the thermal-expansion tensor, J. Appl. Crystallogr. 31 (1998) 748-757.
[17] P. Negrier, L.C. Pardo, J. Salud, J.L. Tamarit, M. Barrio, D.O. Lopez, A. Wurflinger, D. Mondieig, Polymorphism of 2,2-dichloropropane: Crystallographic characterization of the ordered and disordered phases, Chem. Mater. 14 (2002) 1921-1929.
[18] B. Parat, L.C. Pardo, M. Barrio, J.L. Tamarit, P. Negrier, J. Salud, D.O. López, D. Mondieig, Polymorphism of $CBrCl_3$, Chem. Mater. 17 (2005) 3359-3365.
[19] A. Authier, (Ed.), International tables for crystallography D: physical properties of crystals, Kluwer, Dordrecht (NL), 2006.
[20] R.I. Belousov, S.K. Filatov, Glass Phys. Chem 33 (2007) 271-275.
[21] B. Nicolaï, N. Mahé, R. Céolin, I.B. Rietveld, M. Barrio, J.-L. Tamarit, Tyrosine alkyl esters as prodrug: the structure and intermolecular interactions of l-tyrosine methyl ester compared to l-tyrosine and its ethyl and n-butyl esters, Struct. Chem. 22 (2011) 649-659.
[22] A.D. Fortes, I.G. Wood, K.S. Knight, The crystal structure and thermal expansion tensor of MgSO4-11D(2)O(meridianiite) determined by neutron powder diffraction, Phys. Chem. Miner. 35 (2008) 207-221.
[23] P. Negrier, M. Barrio, J.L. Tamarit, N. Veglio, D. Mondieig, Structure of Phase III and Polymorphism of $(CH_3)_3CBr$, Cryst Growth Des 10 (2010) 2793-2800.
[24] I.B. Rietveld, M. Barrio, J.-L. Tamarit, B. Nicolaï, J. Van de Streek, N. Mahé, R. Céolin, B. Do, Dimorphism of the Prodrug L-Tyrosine Ethyl Ester: Pressure-Temperature State Diagram and Crystal Structure of Phase II, J. Pharm. Sci. 100 (2011) 4774-4782.
[25] B. Nicolaï, I.B. Rietveld, M. Barrio, N. Mahé, J.-L. Tamarit, R. Céolin, C. Guéchot, J.-M. Teulon, Uniaxial negative thermal expansion in crystals of tienoxolol, Struct. Chem. 24 (2013) 279-283.
[26] B.T. Goodman, W.V. Wilding, J.L. Oscarson, R.L. Rowley, A note on the relationship between organic solid density and liquid density at the triple point, J. Chem. Eng. Data 49 (2004) 1512-1514.
[27] W. Kauzmann, The Nature of the Glassy State and the Behavior of Liquids at Low Temperatures, Chem. Rev. 43 (1948) 219-256.

Figure

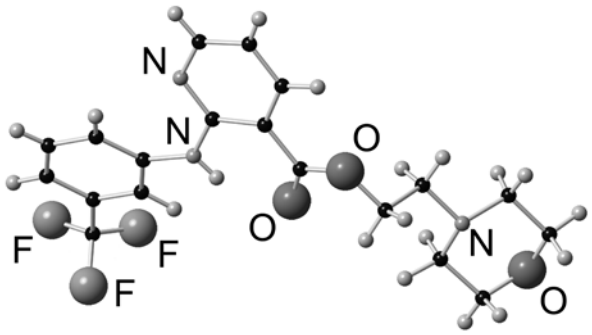

Figure 1. Molecular structure of morniflumate [8] $C_{19}H_{20}F_3N_3O_3$, M_w = 395.38 g mol^{-1}, black spheres are carbon atoms and light grey spheres are hydrogen atoms, oxygen, nitrogen and fluor atoms have been labeled in the figure.

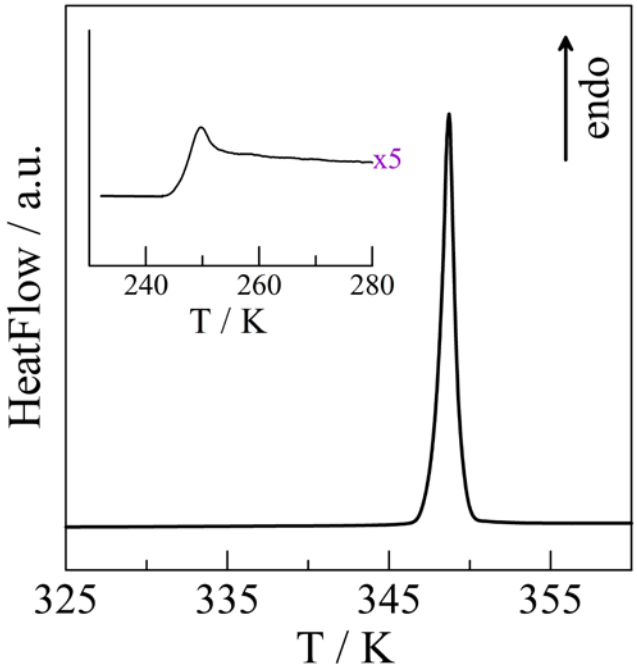

Figure 2. The melting peak and after cooling and reheating the glass transition of morniflumate as obtained by differential scanning calorimetry at a heating rate of 2 K min^{-1}.

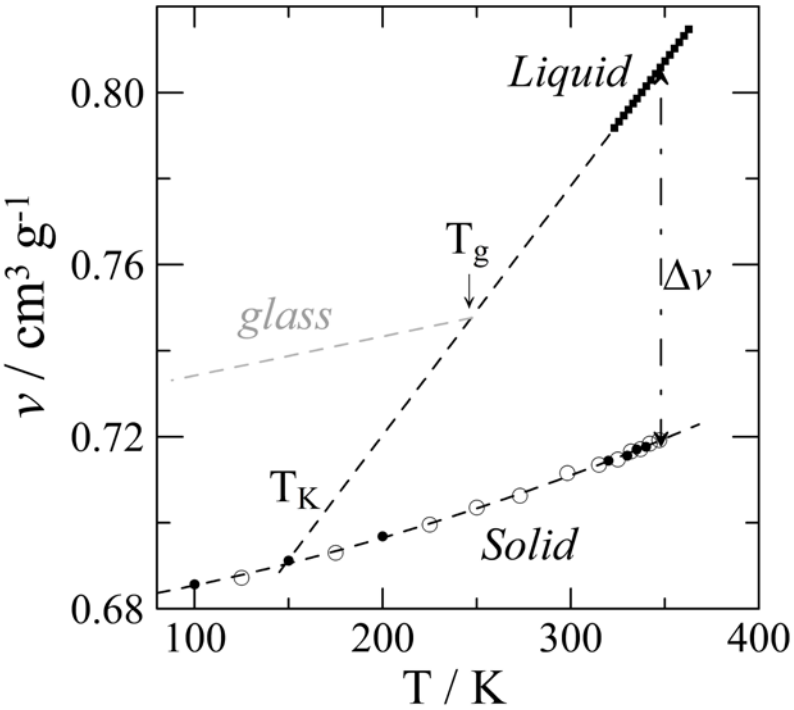

Figure 3. Temperature dependence of the specific volume of crystalline (filled circles: first sample, open circles: second sample) and molten morniflumate (filled squares). The dashed lines through the symbols represent the respective fits, eqs. 2 and 3. The light grey dashed line parallel to the specific volume of the crystalline phase represents the hypothetical specific volume of the glass phase starting at the glass transition temperature $T_g \approx 248$ K. T_k is the Kauzmann temperature at which the v_{liq} of the metastable liquid paradoxically becomes the same as that of the crystalline solid.

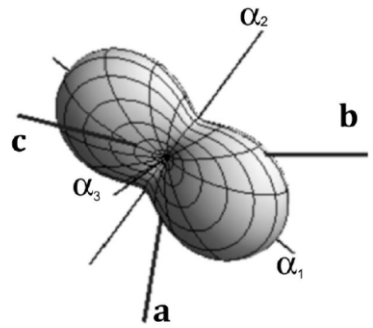

Figure 4. Illustration of the isobaric thermal expansion tensor at 255 K

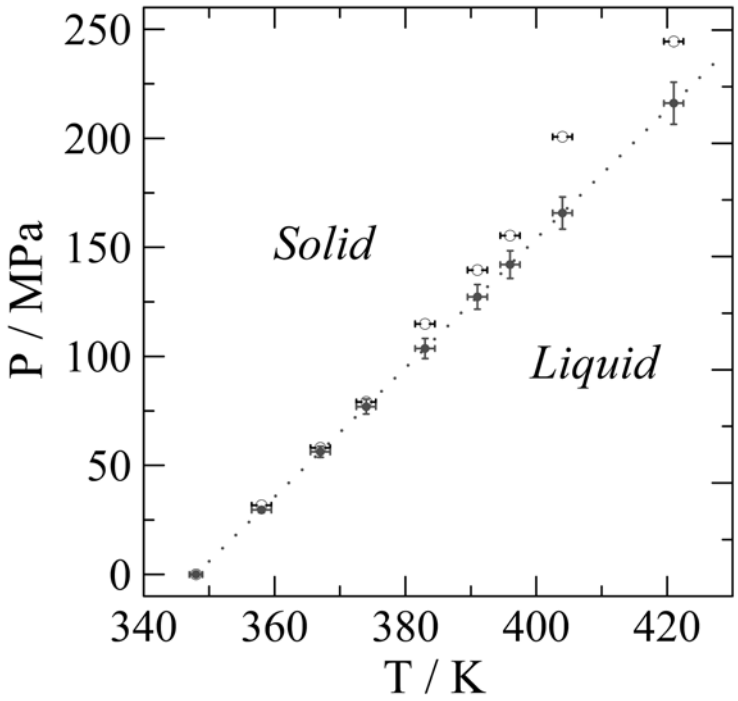

Figure 5. Melting curve of crystalline morniflumate as a function of temperature (*T*) and pressure (*P*). Open circles: experimental HP-DTA values, solid circles: melting data calculated with the Clapeyron equation at the same temperatures as the experimental data (eq. 1). The dotted line is a straight equilibrium line based on the Clapeyron equation. The increasing deviation of the measured data from the straight extrapolation based on the Clapeyron equation is clear, but cannot be easily captured by a second order equation (see text).